Simple prediction method for the edge fracture of steel sheet during vehicle collision (2nd report)

- Edge fracture prediction using CAE -

Kimihito Koyanagi, Kazuyoshi Motomura

Toyota Auto Body Co., Ltd. (Kariya, Aichi, Japan)
Kenichi Watanabe, Mie Tachibana

Kobe steel, Ltd. (Kakogawa, Hyogo, Japan)

Summary:

In the vehicle collisions, prediction accuracy becomes worse because the fracture of the steel sheet generates in the vehicle structure parts and vehicle deformation mode is different from FEM. Consideration of the steel sheet fracture for the improvement in prediction accuracy of vehicle crash simulations is important. On previous paper, it is introduced that prediction method of the fracture limit strain using steel sheets mechanical property obtained from the test-piece tensile test. The 3-point bending tests of the hole attached to a small hat test piece were carried out in this paper and the prediction method is applied to the fracture decision from steel sheet edge of the hat test piece. The 3-point bending test was reproduced in FEM, and it is examined that a fracture decision method by FEM as a fracture limit strain that obtained from prediction method in pervious paper.

Keywords:

Key Words: Safety, CAE, Steel & Iron / FEM, Fracture, Edge

1 Introduction

While CAE technology has been used increasingly in the automobile development process, vehicle collision simulations using CAE has been used extensively, and it is now a critical technology to shorten a vehicle development period and to achieve an advanced balance between a target performance and weight reduction. If any fractures exist in a vehicle structure part at vehicle collisions, a deformation mode of the vehicle collision changes, and it is supposed that the vehicle deformation mode is different from the result of FEM.

Our previous paper (1) reported that the fracture limit strain around hole edges observed in a hole tensile test could be evaluated with a correlation equation using general mechanical properties of steel sheet. For the purpose to develop an effective method for predicting accurately the fracture from hole edges, a three-point bending test was carried out using small hat-shaped test pieces having a hole. It was examined whether the correlation equation was applicable to judge fractures by comparing the strain value when a fracture occurred around the hole edge with the value obtained from the correlation equation. In addition, a FEM model was examined whether to reproduce such a test.

2 Fracture around a hole on three-point bending test

2.1. Test piece and test conditions

Test piece profiles and test conditions are shown in Fig. 1 to Fig. 3. The test piece has a hat-shaped cross section as shown in Fig. 1, which is supported at three points and statically bended by moving the punch upward at the midpoint as shown in Fig. 2. The inner panel has a hole that simulates a hole for mounting a part as shown in Fig. 3.

Representative mechanical properties of the test steel sheet are listed in Table 1. The inner panels used for measuring the fracture limit strain were different from K to O in steel class and thickness, as shown in Table 1.

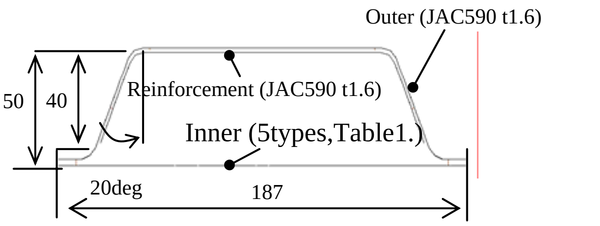

Fig. 1 Profile and cross-section of test piece (unit: mm)

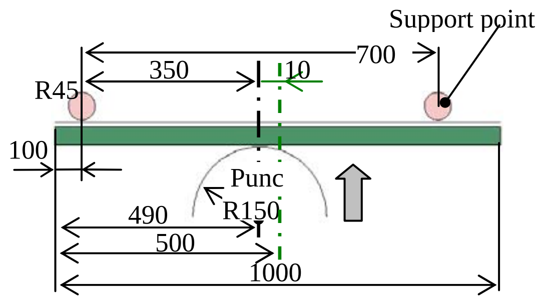

Fig. 2 Test piece and test machine (unit: mm)

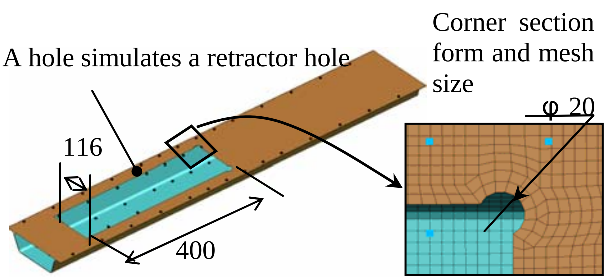

Fig. 3 Profile of retractor hole (unit: mm)

Table1. Combination of inner panel and mechanical properties

No.	Class	t (mm)	YP (Mpa)	TS (Mpa)	EL (%)
K	JAC270D	0.80	153	301	49
L	JAC270D	1.20	181	298	49
M	JAC440W	0.80	325	452	34
N	JAC440W	1.24	407	458	35
O	JAC590 (High Yp)	1.20	458	625	27

The n-number was 3 for each test piece. Load was measured using a load cell attached onto the punch. The fracture limit elongation around the hole was measured as follows. The hole edge area was marked with lines at a 2 mm pitch for a gage length (GL) of 2 mm, and the length was measured at 1 mm away from the edge.

Here, the length between lines across a single pitch before the test is expressed as GL2 (=2 mm), the length across three pitches is as GL6 (=6 mm), both of those after the test are as GL2’ and GL6’ respectively, and the length across a fracture is expressed as δ.

Then, the lengths after subtracting δ from GL2' and GL6' were compared with GL2 and GL6. The results were the elongations for each gauge length, respectively. Fig. 4 shows the measurement position for the elongation.

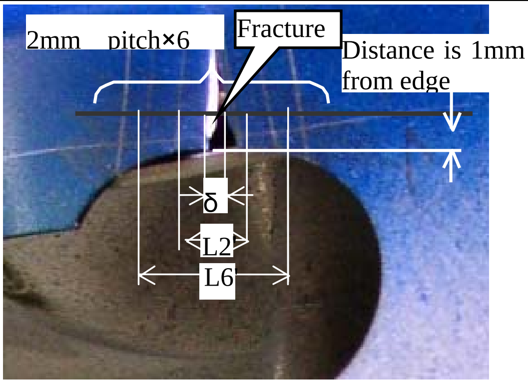

Fig4.Measurement mark-off line of test piece around corner section (after test)

2.2 Result of three-point bending test and the analysis

The test piece was bended in a deformation mode of three-point bending and it broke at the section pressed upward by the punch (Fig. 5). A fracture occurred around the hole edge on the tension side inner panel; on the contrary, the sidewall was folded on the compression side (Fig. 6). Fig. 7 shows the load vs. displacement for all test pieces.

Fig5.Test piece general view (after test)

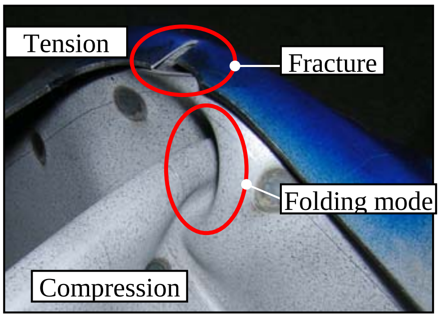

Fig6.Apperance around retractor hole (Test Piece M)

The load increases to the maximum where a bending buckling occurs, and then decreases gradually afterward.

The load at buckling tends to increase as the inner panel material strength increases. However, the differences in the deformation load after bucking among the test pieces were not as much as those in the maximum load. The chain double-dashed lines in the figure indicate the stroke where a fracture occurred around the hole edge. The load did not decrease significantly after fractured from the hole edge. These results mean that the collapsing load after bucking is not influenced so much from the tension side.

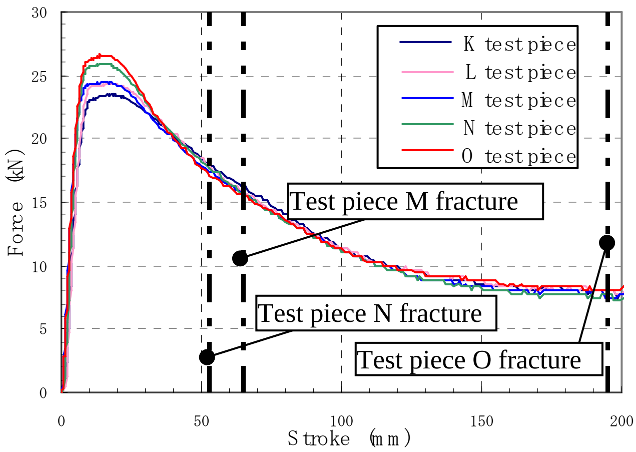

Fig7.Force-displacement curve of test pieces

Displacements when a fracture occurred around the hole edge, and elongations around the hole edge for a gauge length of 2 mm are listed in Table 2 for each test piece. These displacements and elongations are averaged out of n=3 for each test piece.

No fracture occurred on test pieces K and L, which had a good elongation property (large EL50). With test pieces M, N and O that a fracture observed, the fracture occurred not so easily as the material strength increased.

Table2. Displacement at fracture & elongation around hole edge

No	K	L	M	N	O
Average displacement at fracture (mm)	No fracture	No fracture	65	53	195
GL2 average elongation of hole edge (%)	86	72	43	62	59

2.3. Verifying the fracture elongation from hole edge by a three-point bending test using hat-shaped test pieces

Elongations of the hat-shaped test piece at fracture were compared with those elongations obtained from the correlation equation (1) specified in our previous report. The correlation equation, which determines the fracture limit elongation around the hole edge for GL2, EL_{H2}, using the hole expansion ratio λ that is a general mechanical property of steel sheet, and the total elongation EL50 that is obtained from the JIS No. 5 tensile test, is expressed as follows. Where, a, b and c are coefficients to indicate the contribution of each property, which may vary depending on the hole processing history. These test pieces have a hole processed by piercing; therefore, the relevant values for the piercing were applied.

$$EL_{H2} = a \times \lambda^{b} \times EL50^{c} \qquad (1)$$

Fig. 8 shows the comparison of the test results and the calculated fracture elongation around the hole edge. No fracture occurred on test pieces K and L that the elongation around the hole edge was less than the calculated value, whereas a fracture was observed on test pieces M, N and O that the elongation around the hole edge was closed to or exceeded the calculated value. These results proved that the elongation when a fracture occurred around the hole edge on a structure part like the hat-shaped test piece could be obtained from a correlation equation using mechanical properties of steel sheet, and the facture from the hole edge could be predicted.

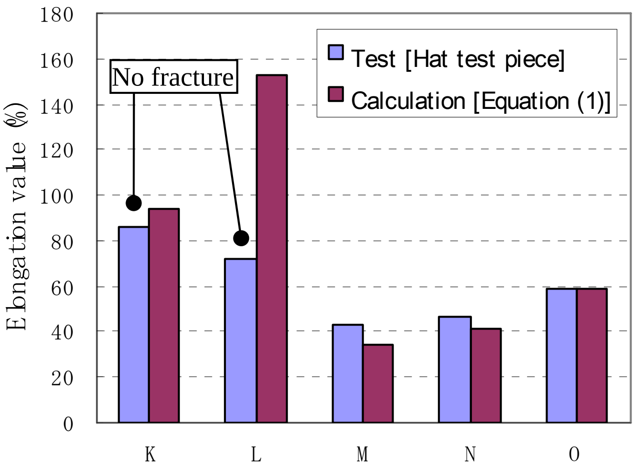

Fig.8 Fracture elongation test and calculation

3 Prediction using FEM

3.1. Modeling the test pieces and other test equipment

In order to examine whether the fracture from the hole edge on a structural part can be evaluated using FEM, the hat-shaped test piece, punch, and test jig were modeled with complete integral shell elements. Fig. 9 shows the mesh size and geometry.

LS-DYNA ver.970 was used as a solver. The punching speed was set to 500 mm/s for the range of displacement up to 15 mm, then to 4000 mm/s at displacement of 60mm, and to be constant afterward. The stress-strain curves measured on the test pieces of each material were used as the material properties; however, the strain rate was not taken into consideration. The stroke was measured with the punch displacement, while the load was measured with the contact force between the punch and test piece.

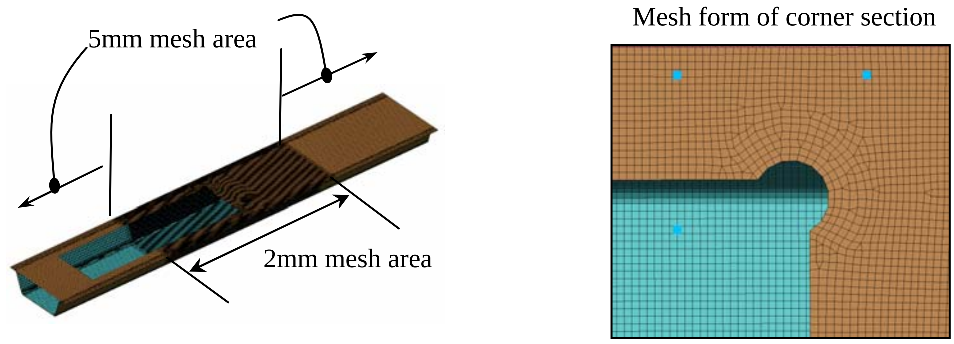

Fig.9 FEM model

3.2. Comparison of FEM results and test results

Among the test pieces that fractured around the hole edge, test results of test piece M were compared with the relevant FEM results. Fig. 10 and Fig. 11 show the comparison of the deformation mode of both the test results and the FEM. Fig. 12 shows the load-displacement curves of both the test results and the FEM.

The FEM reproduces the local deformation, and the maximum load deviates as less as 3%. Thus, it almost accurately reproduces the testing conditions.

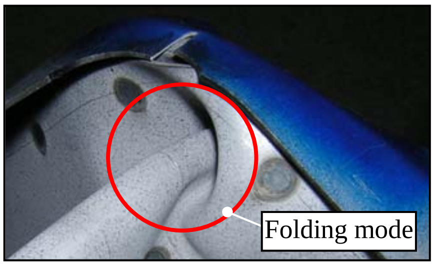

Fig.10 Deformation of experiment around retractor hole (Exp. Test piece M)

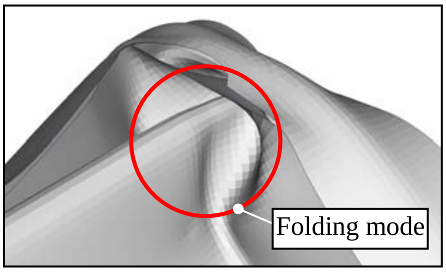

Fig.11 Deformation of FEM around retractor hole

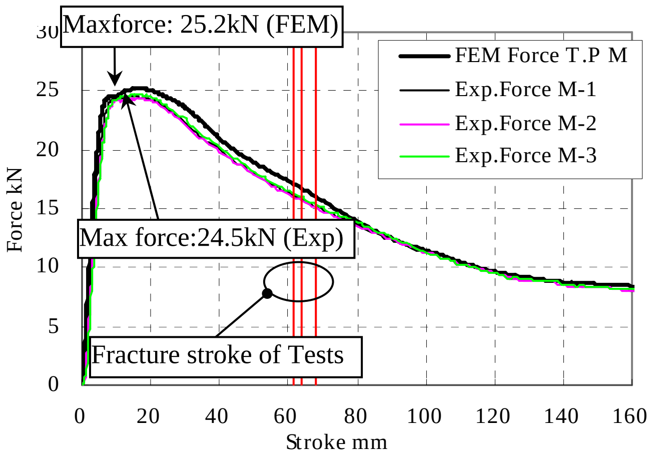

Fig12.Force - displacement curve of Test Piece M (Test & FEM)

3.3. Comparison of strain around the hole edge

The strain around the hole edge obtained from the test was compared with those from the FEM analysis. In the FEM model, the strain was measured in the shell elements correspond to the section

where the elongation was measured in the test. These strain values are the equivalent plastic strain that occurs in the relevant elements at the stroke when a fracture was observed in the test.
Such strain values were compared with the elongation in the test results after converted it into logarithm strain. The strain was measured in elements (1), (2) and (3) shown in Fig. 13.
The GL2 strain value measured in the test was compared with the equivalent plastic strain values in element (2), while the GL6 strain value was compared with the equivalent plastic strain value averaged over elements (1) to (3).

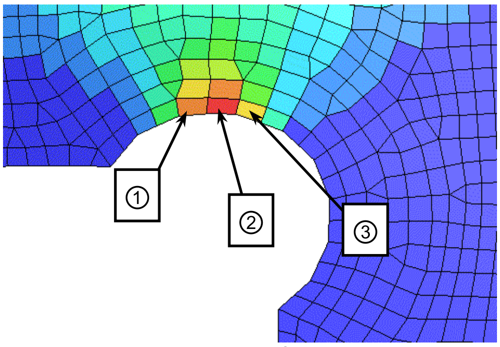

Fig13. Measurement element of FEM model around corner section

Fig. 14 and Fig. 15 show the comparison of the strain values when a fracture occurred around the hole edge on hat-shaped test pieces. For both gauge lengths of GL2 and GL6, the strain measured in the test is closed to those by the FEM; therefore, this model is evaluated to be reproducing accurately the strain concentration around the hole edge.

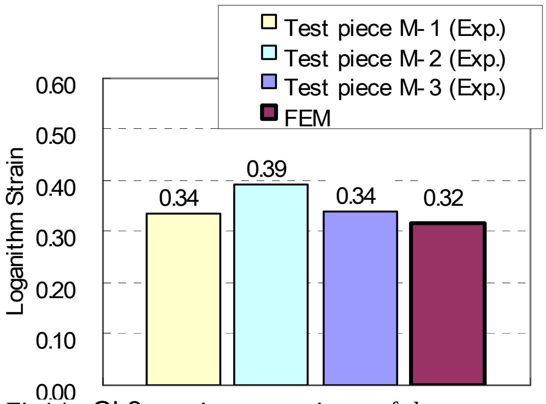

Fig14. GL2 strain comparison of hat type test piece (Test & FEM)

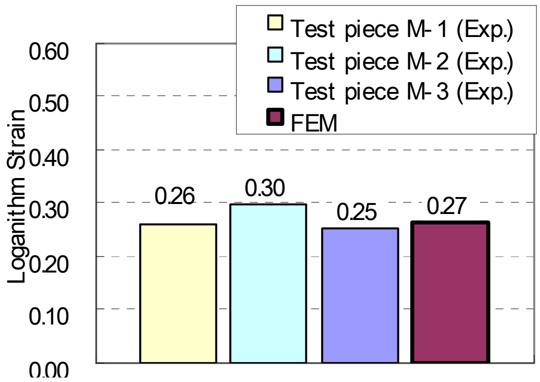

Fig15. GL6 strain comparison of hat type test piece (Test & FEM)

4 Conclusion

A three-point bending test using hat-shaped test pieces was carried out along with the corresponding FEM analysis. The load-displacement curve and the strain around a fracture measured in the test were compared with those by the FEM analysis. It can be concluded as follows.

(1) The fracture limit strain value calculated from a correlation equation using mechanical properties of sheet steel is applicable as a fracture limit strain value for a structure part like the hat-shaped test piece. This approach may be effectively used to predict the fracture from the hole edge on a structural part.

(2) The local strain concentration around a hole edge can be reproduced using a FEM model proposed in this paper, which may predict the fracture from hole edges.

This paper is reprinted from JSAE Anual congress (spring) proceedings No 20065103

5 Reference

(1) Kenichi Watanabe, etc. Simple prediction method for the edge fracture of steel sheet on the vehicle collision (1st report), JSAE Paper No. 20065803

